International Journal of Heat and Mass Transfer 79 (2014) 64–71

Contents lists available at ScienceDirect

International Journal of Heat and Mass Transfer

journal homepage: www.elsevier.com/locate/ijhmt

Thermal conductivity and contact resistance of mesoporous silica gel adsorbents bound with polyvinylpyrrolidone in contact with a metallic substrate for adsorption cooling system applications

Amir Sharafian, Khorshid Fayazmanesh, Claire McCague, Majid Bahrami *

Laboratory for Alternative Energy Conversion (LAEC), School of Mechatronic Systems Engineering, Simon Fraser University, BC V3T 0A3, Canada

ARTICLE INFO

Article history:
Received 26 June 2014
Received in revised form 19 July 2014
Accepted 27 July 2014
Available online 20 August 2014

Keywords:
Adsorption cooling systems
Thermal conductivity
Thermal contact resistance
Silica gel
Polyvinylpyrrolidone

ABSTRACT

Silica gel bound with polyvinylpyrrolidone (PVP) is a new composite adsorbent with promising uptake rate designed for adsorption cooling systems. In this study, the thermal conductivity of silica gel-PVP and its thermal contact resistance (TCR) with a metallic substrate are measured using the guarded-hot plate apparatus under vacuum pressure. This study sheds light on the importance of TCR at the interface between the adsorbent and substrate, which has been overlooked in most studies in the literature. The measurements show that the thermal conductivity of silica gel-PVP adsorbent is 0.26 W/m/K which is 78.6% higher than that of dry silica gel packed bed. Also, the analysis indicates that the TCR between the adsorbent and metallic substrate is between 1.29–3.80 K/W which is equivalent to 0.20–0.69 mm of adsorbent thickness. Finally, the results indicate that the ratio of total TCR between the adsorbent and metallic substrate is up to 26% of the adsorbent-metallic substrate bulk resistance.

1. Introduction

Since 1960s, motor vehicles' fuel consumption in the U.S. has steadily increased by 4.2 times [1] contributing to air pollution, ozone depletion, and global warming. The main auxiliary load in light-duty vehicles comes from air conditioning (A/C) system in which a compressor draws power from the vehicle's internal combustion engine (ICE). During the SFTP-SC03 [2] driving cycle, which represents the engine load and gas emissions due to the use of A/C systems in light-duty vehicles, using a vapor compression refrigeration cycle (VCRC) increases fuel consumption by 28%, and CO_2 and NOx emissions by 71% and 81%, respectively. A VCRC compressor can add up to 5–6 kW peak power draw on a vehicle's ICE [3]. This auxiliary power consumption is equivalent to the power required for a 1200-kg sedan cruising at 56 km/h [3]. Moreover, in a typical ICE, almost 70% of the total fuel energy is dissipated through the engine coolant and the ICE exhaust gas in the form of waste heat. A promising alternative of conventional VCRCs could be adsorption cooling systems (ACS), which have received attention in the recent years motivated by higher fuel prices, energy shortages, and government environmental/emission regulations [4–6]. Therefore, proper implementation of the ACS in vehicles can significantly reduce fuel consumption and minimize carbon footprint of vehicles.

Working pairs in ACS are a combination of an adsorbent, e.g. zeolite, silica gel, and activated carbon, and an adsorbate, e.g. water, methanol, and ammonia. Most of these working pairs, such as zeolite-water, silica gel-water and activated carbon-methanol, are environmentally friendly, non-toxic, non-corrosive, non-ozone depleting, and inexpensive compared to conventional refrigerants, such as chlorofluorocarbons (CFCs), hydrochlorofluorocarbons (HCFCs), and hydrofluorocarbons (HFCs) [7]. Also, ACS is quiet and has no-moving parts except the valves. Thus, ACS is ideal candidates for vehicle A/C systems. However, commercialization of ACS faces major challenges because of (i) low specific cooling power (SCP), which is defined as the ratio of cooling load to the mass of dry adsorbent multiplied by the cycle time; and (ii) poor coefficient of performance (COP).

The low thermal conductivity of the adsorbent particles (∼0.1–0.4 W/m/K) [8–10] and low mass diffusivity of adsorbent-adsorbate pairs ($\sim10^{-8}$–10^{-14} m^2/s) [9,11] result in a heavy and bulky ACS. The thermal conductivity of dry silica gel packed bed is summarized in Table 1. The experimental data in Table 1 show that

---

* Corresponding author. Address: School of Mechatronic Systems Engineering, Simon Fraser University, # 4300, 250-13450 102nd Avenue, Surrey, BC V3T 0A3 Canada. Tel.: +1 (778) 782 8538; fax: +1 (778) 782 7514.

E-mail addresses: asharafi@sfu.ca (A. Sharafian), kfayazma@sfu.ca (K. Fayazmanesh), clairem@sfu.ca (C. McCague), mbahrami@sfu.ca (M. Bahrami).

http://dx.doi.org/10.1016/j.ijheatmasstransfer.2014.07.086
0017-9310/© 2014 Elsevier Ltd. All rights reserved.

Nomenclature

A	cross-sectional surface area (m^2)
A/C	air conditioning
ACS	adsorption cooling system
COP	coefficient of performance
ΔT	temperature difference (K)
ICE	internal combustion engine
k	thermal conductivity (W/m/K)
L	length (m)
PVP	polyvinylpyrrolidone
$\dot{Q}$	heat flow (W)
R	thermal resistance (K/W)
SCP	specific cooling power (W/kg)
t	thickness (m)
TCR	thermal contact resistance (K/W)
THS	transient hot-strip
THW	transient hot-wire
VCRC	vapor compression refrigeration cycle
W	width (m)
Subscripts	
ads	adsorbent layer
ads-metal	adsorbent layer and metallic substrate
flux	fluxmeter
flux-metal	fluxmeter and metallic substrate
metal	metallic substrate
sample	prepared sample

the thermal conductivity of dry silica gel is low and varies with bed density.

To increase the heat transfer rate to adsorbent particles, several solutions were proposed in the literature such as mixing and consolidating adsorbent particles with expanded graphite, carbon fiber, metal foam and aluminum hydroxide [20]. However, consolidation of adsorbent particles results in decreasing permeability of adsorbate through the adsorbent particles. As such, finding alternative solutions to enhance both heat and mass transfer rates are preferred.

Recently, a new mesoporous silica gel adsorbent with polyvinylpyrrolidone (PVP) binder was prepared and characterized in our group, Laboratory for Alternative Energy Conversion (LAEC), with high water uptake capacity. Instead of consolidating the silica gel which reduces the permeability of adsorbate or adding metal foam which increases the weight of adsorbent, the silica gel particles bound with PVP. This polymeric binder improves the contact between the silica gel particles and increases water uptake capacity of adsorbent due to its hydrophilic nature. Also, PVP helps the silica gel particles to adhere to the metallic substrate and increases heat transfer rate. This study will shed light on the importance of thermal contact resistance (TCR) at the interface between the adsorbent and substrate, which has been overlooked in most studies in the literature. TCR is an interfacial phenomenon and is fundamentally different from thermal conductivity, which is a bulk property and thus should be treated separately. To show the impact of the TCR, several silica gel-PVP adsorbent samples with the bulk density of 450–520 kg/m^3 were prepared and coated on a metallic substrate and its thermal conductivity and TCR are measured. It is observed through experiments that the TCR forms up to 13% of the total thermal resistance, and therefore, should be included in the design and analysis of adsorber beds.

2. Pertinent literature

Several methods were used in the literature to find the thermal conductivity of adsorbent materials. Gustafsson et al. [21] developed a transient hot-strip (THS) method to measure the thermal conductivity and the thermal diffusivity of solids and fluids with low electrical conductivity. In this method, the metal strip, which functions as a heat source, is placed between two slabs of the solid material. The THS method has better accuracy than the transient hot-wire (THW) method because for many solid materials, such as porous materials, the metal strip has better contact for transferring heat to the material than the wire [21]. The THS method was used to measure the thermal conductivity of moist silica gel by Bjurström et al. [12]. They measured the thermal conductivity of moist silica gel under different porosity, water content, water vapor pressure and silica gel temperature. Bjurström et al. [12] indicated that the thermal conductivity of the moist silica gel bed increased from 0.147 to 0.265 W/m/k by increasing the water content from 0 to 0.329 kg/kg, respectively.

Sarwar and Majumdar [22] developed an analytical model to predict the effective thermal conductivity of wet composite porous media as a function of porosity and water content. They added the effects of water content to the unit cell model proposed by Dul'Nev [23] and Luikov et al. [24]. Sarwar and Majumdar [22] showed that their model can predict the experimental data reported by Bjurström et al. [12] with maximum relative difference of 21%.

The thermal conductivity of composite silica gel and $CaCl_2$ was measured by Tanashev and Aristov [25,26] using the THW method at 20°C. Their results indicated that the effective thermal conductivity of silica gel and $CaCl_2$ increased from 0.112 to 0.153 W/m/K by increasing the water content of the composite adsorbent from 0.01 to 0.34 kg/kg [25]. They concluded that

Table 1
Thermal conductivity packed bed of dry silica gel reported in the literature [12].

Ref.	Particle density (kg/m^3)	Bed density (kg/m^3)	Effective thermal conductivity (W/m/K)	Mean temperature (°C)
Mantell [13]	1201	720	0.144	–
Nienergall [14]	–	–	0.198	–
Vasilev et al. [15]	–	850	0.153	20
	–	998	0.182	20
	–	865	0.160	20
Sharma et al. [16]	891	452–750	0.128–0.168	20–135
Sharma and Hughes [17]	–	428–690	0.116–0.148	48.7
Blasinski and Heim [18]	870	461–609	0.106–0.135	140
Simonova [19]	–	634	0.151	20
	–	838	0.179	20

changes in the effective thermal conductivity of composite silica gel and $CaCl_2$ at water contents less than 0.4 kg/kg were negligible. In a real ACS, the water content of silica gel is less than 0.4 kg/kg because silica gel cannot uptake water beyond 0.4 kg/kg during short cycle times ($\sim$10–20 min) [27,28]. Thus, the assumption of constant thermal conductivity for composite silica gel and $CaCl_2$ in an ACS can be a good approximation.

Tamainot-Telto and Critoph [9] measured the effective thermal conductivity of monolithic carbon by using the guarded-hot plate device which is a standard method for determining the steady state thermal conductivity of materials [9]. The effective thermal conductivity of monolithic carbon was reported between 0.349–0.4455 W/m/k. However, the monolithic carbon had permeability of 10^{-14} m^2/s [9] which significantly reduces the adsorbate penetration depth through the monolithic carbon. The other point, which was neglected in Tamainot-Telto's and Critoph's [9] measurements, was the TCRs between the heat source and sink, and the sample.

Freni et al. [10] measured the thermal conductivity of composite silica gel and $CaCl_2$ bound with aluminum hydroxide by using the THW method under different water vapor pressure and temperature, and water content. Their results showed that the effects of vapor pressure and temperature were negligible on the thermal conductivity of the composite adsorbent. However, the effective thermal conductivity of silica gel and $CaCl_2$ increased from 0.12 to 0.227 W/m/K by increasing the water content from 0.05 to 0.28 kg/kg dry adsorbent, respectively. Critoph and Zhong [29] summarized the thermal conductivity of a wide range of adsorbents reported in the literature, Table 2.

It can be seen in Table 2 that the composite adsorbents with expanded graphite [30,31,34–36] resulted in higher thermal conductivities. These experiments were performed under atmospheric pressure and unsteady thermal conductivity measurement methods, e.g. THW or THS methods. Adsorption process is an exothermic process and adsorbent particles adsorb the air humidity and generate heat. Therefore, the measured temperature difference in the unsteady thermal conductivity measurement methods is less than that of with no adsorption [37]. To reduce this misleading error, Wang et al. [37,38] measured the thermal conductivity of the consolidated expanded natural graphite slab using the guarded-hot plate apparatus. Their measurements indicated that the thermal conductivity of the consolidated adsorbent increased from 1.4 to 1.7 W/m/K by increasing its density from 200 to 500 kg/m^3, respectively. However, Wang et al. [37,38] did not excluded the effects of TCR in their calculations.

In all above mentioned studies, two main parameters were neglected which can considerably affect the results: (i) thermal conductivity measurement under atmospheric pressure, and (ii) including TCR in the thermal conductivity calculations. It should be noted that TCR is an interfacial phenomena and is a function of compression (pressure), surface characteristics (e.g. roughness, out-of-flatness) and bonding of the adsorbent with the substrate whereas conductivity is a bulk property and depends on the material microstructure and composition. Due to the low thermal conductivity and high porosity of adsorbent materials, the TCR cannot be neglected in the measurements and it should be excluded from the thermal resistance of adsorbent. Also, adsorbents adsorb air humidity and generate heat. As a result, the measured temperature difference is smaller than where there is no adsorption process. To cancel these errors, the thermal conductivity of adsorbent materials should be measured under vacuum pressure and the TCR effect should be treated separately and de-convoluted from the conductivity measurements.

Table 2
Thermal conductivity of different adsorbents reported in literature [29].

Adsorbent material	Thermal conductivity (W/m/K)	Density (kg/m^3)	Ref.
Expanded graphite–metal chloride	10–40	–	[30]
Expanded graphite–zeolite 13×	5–15	–	[31]
Consolidated zeolite 4A	0.3	960	[32]
Consolidated zeolite 4A+ adhesive bond to the wall	0.3	960	[32]
Consolidated zeolite 13×	0.58	–	[33]
Expanded graphite (20–30%) – silica gel	10–20	–	[34,35]
Silica gel – $CaCl_2$	0.12–0.22	–	[10]
Monolithic carbon	0.35–0.44	750	[9]
Expanded natural graphite – silica gel	3.7–19.1	38–286	[36]

3. Sample preparation

Silica gel bound with PVP sample was prepared utilizing chromatography-grade commercial silica gel with irregular-shaped grains (0.2–0.5 mm) and average pore diameter of 9 nm supplied from Silicycle, Inc (Quebec, Canada). In batches of 100 g, the dry mesoporous silica gel was mixed with PVP. The mixture was baked at 200°C until judged dry by consistent weight measurements.

4. Thermal conductivity measurement

4.1. Test bed

A custom-built thermal conductivity measurement test bed was used to measure the thermal conductivity of the prepared samples. The test bed and schematic of sample location between two fluxmeters are shown in Fig. 1. The test bed is designed based on the guarded-hot plate apparatus recommended by ASTM standard C177-13 [39]. The test column is housed under a glass vacuum chamber which is connected to a vacuum pump to evacuate the chamber during the experiments. Further details of the test bed are explained elsewhere [40,41].

The two-thickness method is used to measure the sample thermal conductivity and de-convolute the effect of TCR between the fluxmeters and sample. This method is a precise method to exclude the TCR from the thermal conductivity of the sample.

4.2. Test procedure

To measure the thermal conductivity of silica gel-PVP adsorbent, two experiments were designed as shown in Fig. 2.

Fig. 2a shows the first method to find the thermal conductivity of the composite adsorbent and TCR between the adsorbent and metallic substrate. The thermal resistance network of this sample is shown in Fig. 2a. Heat, $\dot{Q}$, passes through the top fluxmeter, different thermal resistances and the bottom fluxmeter. To find the thermal resistances, the thermal conductivity of a bare metallic substrate, copper was used in our experiments, should be measured separately to find the metallic substrate resistance, R_{metal}, and the TCR between the fluxmeter and metallic substrate, $TCR_{flux\text{-}metal}$. The next step is to measure the thermal conductivity of an adsorbent layer, R_{ads}, and the TCR between the adsorbent and metallic substrate, $TCR_{ads-metal}$, by using the two-thickness method. To find the last unknown, $TCR_{ads-metal}$, the whole sample including the adsorbent and metallic substrate should be placed in the thermal conductivity measurement test bed. However, during the preparation of the samples, we noticed that the surface of the prepared samples were not identical and smooth, and as a result, the $TCR_{flux-ads}$ for different samples were not the same. To solve this problem, the silica gel-PVP adsorbent was sandwiched

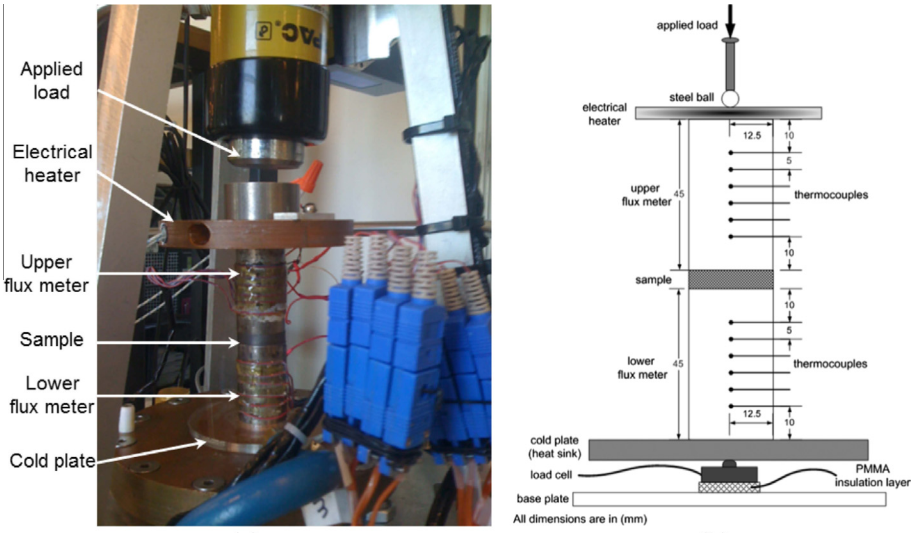

(a) (b)

Fig. 1. (a) Thermal conductivity and TCR measurement testbed, and (b) schematic of sample location, fluxmeters and thermocouples in the testbed [40,41].

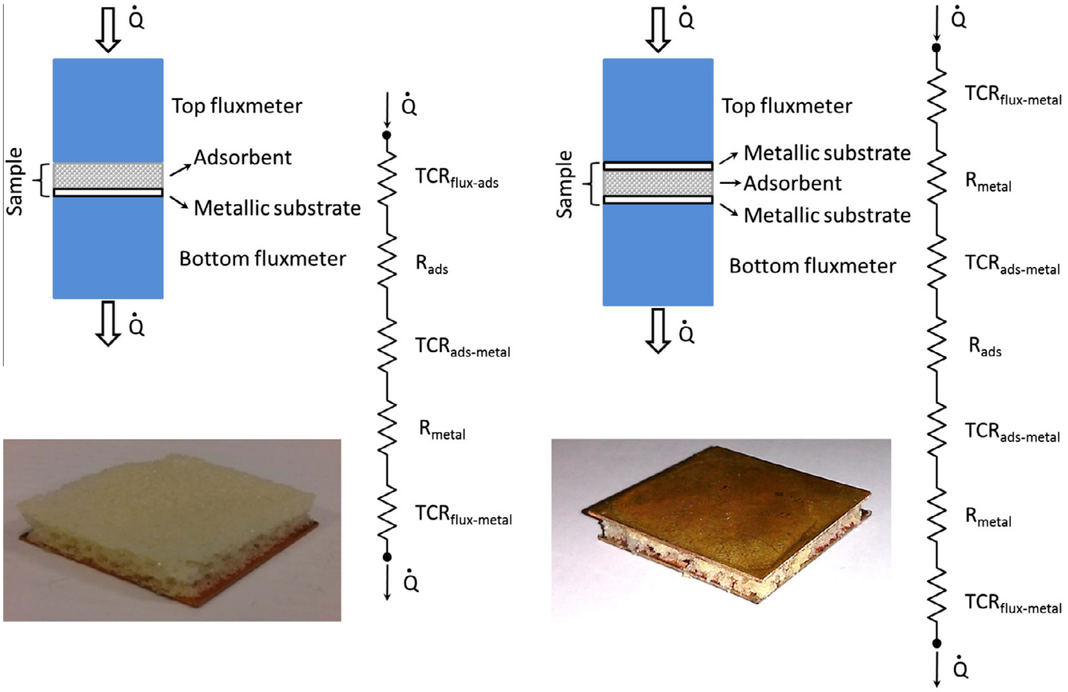

(a) (b)

Fig. 2. Prepared samples and resistance network to measure the thermal conductivity of silica gel bound with PVP and TCR between the sample and metallic substrate: (a) adsorbent on a metallic substrate (copper plate), and (b) adsorbent sandwiched between two copper plates.

between two metallic substrates, as shown in Fig. 2b. Similar to the previous procedure, R_{metal} and $TCR_{flux-metal}$ should be measured separately by using a bare metallic substrate. Then, the two-thickness method can be used to find the R_{ads} and $TCR_{ads-metal}$. Eqs (1)–(6) show the mathematical calculations to find the R_{ads} and $TCR_{ads-metal}$. Eqs (1) and (2) give the bulk resistances of two samples with different thicknesses which were prepared based on Fig. 2b.

$$R_{sample\,1} = 2TCR_{flux-metal} + 2R_{metal} + 2TCR_{ads-metal} + R_{ads,1} \tag{1}$$

$$R_{sample\,2} = 2TCR_{flux-metal} + 2R_{metal} + 2TCR_{ads-metal} + R_{ads,2} \tag{2}$$

By subtracting Eq. (1) from Eq. (2),

$$R_{sample\,2} - R_{sample\,1} = R_{ads,2} - R_{ads,1} \tag{3}$$

where, $R_{ads,1}$ and $R_{ads,1}$ are the adsorbent resistance with different thicknesses and are equal to $\frac{t_{ads,1}}{k_{ads}A}$, $\frac{t_{ads,2}}{k_{ads}A}$, respectively. t_{ads}, k_{ads} and A refer to the adsorbent thickness, thermal conductivity, and cross-sectional surface area, respectively. $R_{sample\,1}$ and $R_{sample\,2}$ are calculated from Eqs. (4) and (5):

$$R_{sample\,1} = \frac{\Delta T_1}{\dot{Q}_1} \tag{4}$$

$$R_{sample\,2} = \frac{\Delta T_2}{\dot{Q}_2} \tag{5}$$

where, $\dot{Q}$ and ΔT are the heat transfer rate that passes through the fluxmeters and temperature difference between two sides of the sample, respectively. By substituting Eqs. (4) and (5) in Eq. (3), the thermal conductivity of composite adsorbent can be determined.

$$k_{ads} = \frac{t_{ads,2} - t_{ads,1}}{A(R_{sample\,2} - R_{sample\,1})} \quad (6)$$

As shown in Eq. (6), the thermal conductivity of adsorbent can be calculated by using the two-thickness method and de-convoluting the TCR between different layers. The TCR between the adsorbent and metallic substrate, $TCR_{ads-metal}$, is determined by replacing the measured values in Eqs. (1) or (2).

4.3. Uncertainty analysis

To find the uncertainty during the thermal conductivity and TCR measurements, the relevant parameters to the bulk thermal resistance or thermal conductivity of adsorbent are shown in Eq. (7):

$$k_{ads} = f(\dot{Q}, \Delta T, t, A, k_{flux}) \quad (7)$$

The uncertainty in the thermal conductivity measurements can be calculated similar to the procedure explained by Unsworth et al. [42]. The main uncertainty in the calculations is due to the heat flow that passes through the fluxmeters. The maximum errors in the temperature and length measurements are ±1°C and 0.01 mm, respectively. The fluxmeters have been made out of Armco iron with tolerance in thermal conductivity of ±0.1 W/m/K. Eq (8) gives the total uncertainty in measurements [42].

Table 3
Uncertainty of relevant parameters in the thermal conductivity and TCR measurements.

$\frac{\delta \dot{Q}}{\dot{Q}}$	$\frac{\delta \Delta T}{\Delta T}$	$\frac{\delta t}{t}$	$\frac{\delta A}{A}$	$\frac{\delta k_{flux}}{k_{flux}}$
0.15–0.29	0.018	0.0019	0.00056	0.00139

Table 4
Dimensions of prepared samples.

Sample No.	Thickness (mm)			Heat transfer surface area (m^2)
	Copper plate	Adsorbent	Total	
1	0.762	3.75	5.27	6.45×10^{-4}
2	0.762	6.6	8.12	6.45×10^{-4}

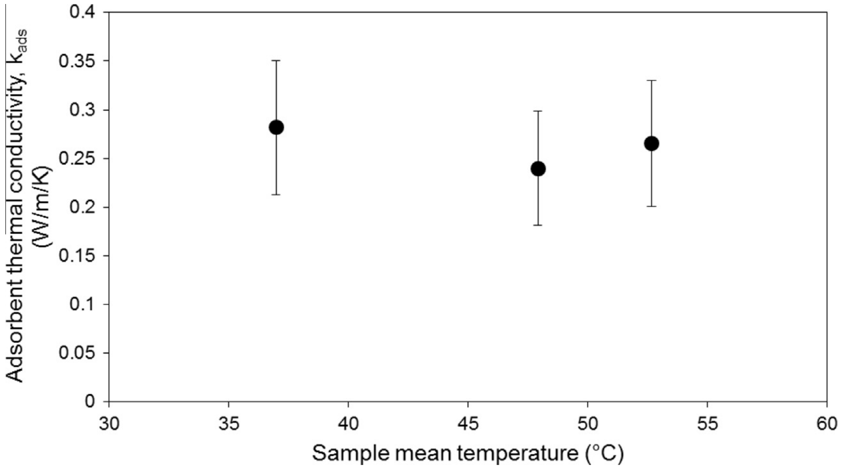

Fig. 3. Thermal conductivity of silica gel bound with PVP vs. sample mean temperature.

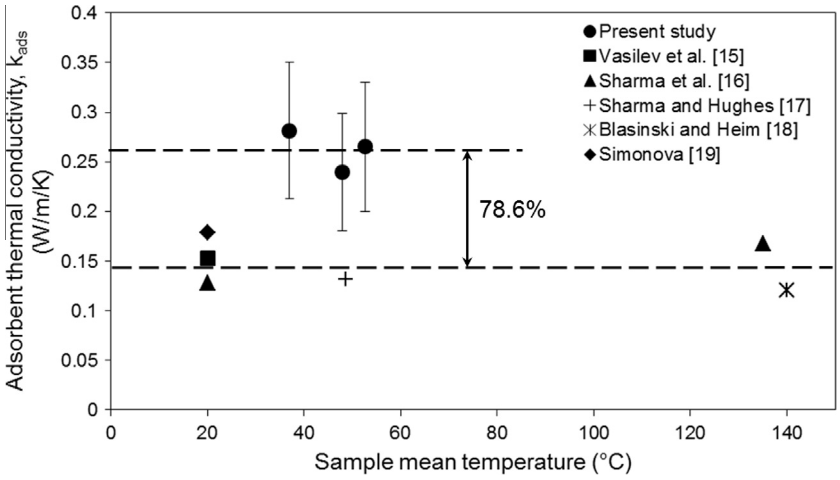

Fig. 4. Comparison between thermal conductivity of silica gel bound with PVP in the present study with those reported for dry silica gel packed bed.

$$\frac{\delta k_{ads}}{k_{ads}} = \sqrt{\left(\frac{\delta \dot{Q}}{\dot{Q}}\right)^2 + \left(\frac{\delta \Delta T}{\Delta T}\right)^2 + \left(\frac{\delta t}{t}\right)^2 + \left(\frac{\delta A}{A}\right)^2 + \left(\frac{\delta k_{flux}}{k_{flux}}\right)^2} \tag{8}$$

where $\frac{\delta \dot{Q}}{\dot{Q}}$ and $\frac{\delta A}{A}$ are calculated as follows [42]:

$$\frac{\delta \dot{Q}}{\dot{Q}} = \frac{1}{2}\frac{\dot{Q}_{top\,flux} - \dot{Q}_{bottom\,flux}}{\dot{Q}_{ave}} \tag{9}$$

$$\frac{\delta A}{A} = \sqrt{\left(\frac{\delta L}{L}\right)^2 + \left(\frac{\delta W}{W}\right)^2} \tag{10}$$

In Eq. (10), L and W are the length and width of the sample, which are equal to 25.4 mm. The uncertainty associated with the adsorbent thermal conductivity and TCR measurements are summarized in Table 3.

By substituting the calculated uncertainties tabulated in Table 3 in Eq. (8), the experiment uncertainty is estimated to be between 15–29% with average uncertainty of 24.5%.

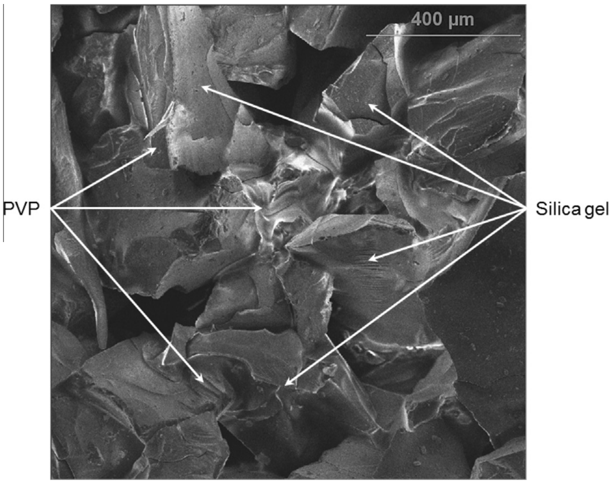

Fig. 5. SEM image of silica gel-PVP adsorbent.

5. Results and discussion

To measure the thermal conductivity of silica gel bound with PVP based on the designed experiment shown in Fig. 2b, two samples were prepared. The dimensions of the prepared samples are summarized in Table 4. The composite adsorbent was placed between two copper plates with 0.762 mm in thickness and baked at 200°C until judged dry by consistent weight measurements.

After running the experiments at different heat transfer rates (thus various temperatures), the thermal conductivity of composite adsorbent were determined by using Eq. (6). Fig. 3 shows the thermal conductivity of composite silica gel vs. sample mean temperature.

As shown in Fig. 3, the thermal conductivity of composite adsorbent varies between 0.24–0.28 W/m/K. The comparison between the measured thermal conductivity in this study and those of reported for the packed bed of dry silica gel is shown in Fig. 4. The experimental data in the literature indicates that the sample mean temperature does not significantly affect the thermal conductivity of silica gel packed bed. Also, the comparison indicates that the average measured thermal conductivity of silica gel bound with PVP is 78.6% higher than those reported in the literature for the packed bed of dry silica gel [15–19].

The reason for the present higher thermal conductivity of silica gel-PVP adsorbent is that the mesoporous silica gel grains are bound with PVP and, as a result, the grains have better connection together. Fig. 5 shows the scanning electron microscope (SEM) image of silica gel-PVP adsorbent. Also, the thermal conductivity measured by Ref. [15–19] did not de-convolute the TCR from the

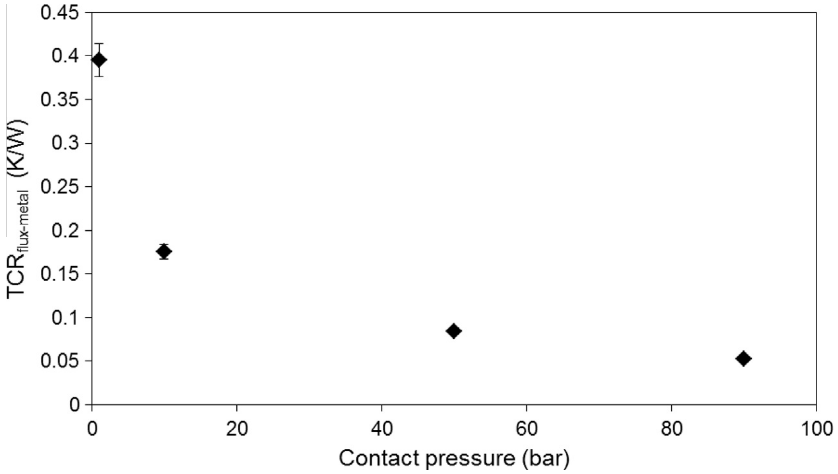

Fig. 6. Thermal contact resistance between fluxmeters and copper plate.

Table 5
Thermal resistance and TCR between different layers of adsorbent layer sandwiched between two metallic substrates, Fig. 2b.

Sample mean temperature (°C)	k_{ads} (W/m/K)	R_{metal} (K/W)	TCR$_{flux\text{-}metal}$ (K/W)	TCR$_{ads\text{-}metal}$ (K/W)	Equivalent adsorbent thickness due to TCR$_{ads\text{-}metal}$ (= TCR$_{ads\text{-}metal} \times k_{ads} \times A$) (mm)
36.98	0.282	0.003	0.395	3.80	0.69
47.93	0.240	0.003	0.395	1.29	0.20
52.68	0.265	0.003	0.395	2.46	0.42

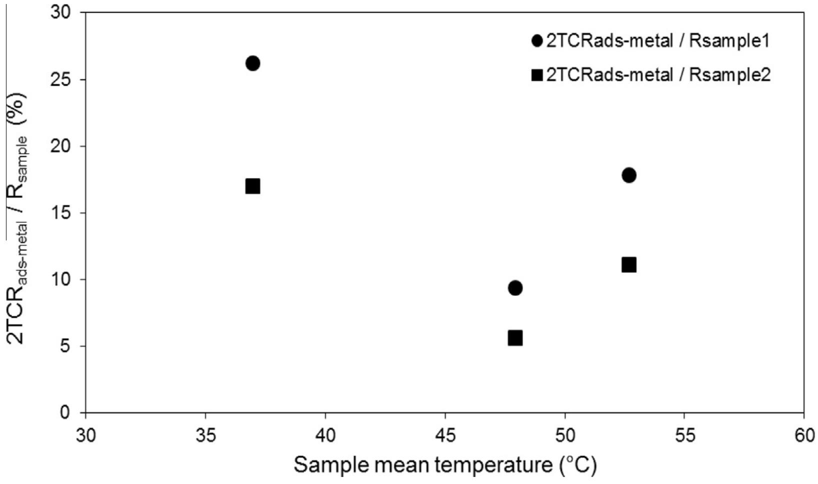

Fig. 7. Ratio of 2TCR$_{ads\text{-}metal}$ to the bulk resistances, $R_{sample\,1}$ and $R_{sample\,2}$ vs. sample mean temperature.

total resistance which results in lower thermal conductivity measurement.

To find the $TCR_{flux-metal}$, a copper (alloy 110) plate with thermal conductivity of 388 W/m/K were selected as the metallic substrate. The TCR between the fluxmeters and copper plate, $TCR_{flux-metal}$, was measured under different contact pressures, Fig. 6.

The maximum uncertainty in the $TCR_{flux-metal}$ measurement was 4.8%. As shown in Fig. 6, the $TCR_{flux-metal}$ reduces by increasing the contact pressure. However, due to the brittle nature of silica gel-PVP adsorbent, it is not possible to increase the contact pressure up to 90 bars. As such, the $TCR_{flux-metal}$ of 0.395 K/W at the contact pressure of 1.3 bar was used in the calculations, the same contact pressure which was applied on the samples during the tests. By substituting the calculated values in Eqs. (1) or (2), the TCR between the adsorbent layer and metallic substrate, $TCR_{ads-metal}$, is calculated. The calculated thermal resistances and TCR in this study are summarized in Table 5.

It can be seen in Table 5 that the $TCR_{ads-metal}$ varies from 1.29–3.80 K/W which is equivalent to 0.2–0.69 mm of the silica gel-PVP thickness. These results indicate that the effects of $TCR_{ads-metal}$ becomes important where the adsorbent thickness is small, e.g., adsorbent coating. The ratio of $2TCR_{ads-metal}$ (there are two TCRs of the adsorbent and metallic substrate in the bulk resistance) to the bulk resistances, $R_{sample\,1}$ and $R_{sample\,2}$, are shown in Fig. 7.

Fig. 7 shows that the effect of two TCRs between the adsorbent layer and substrate to the bulk resistance, $2TCR_{ads-metal}/R_{sample\,1}$, can be as high as 26%. This clearly shows that TCR is significant and cannot be neglected; and should be considered in thermal design and analysis of adsorber beds.

6. Conclusions and final remarks

In this study, the effect of TCR on the overall heat resistance of an adsorbent layer on a metallic substrate was studied experimentally. To demonstrate the impact of TCR, silica gel bound with PVP samples were coated on copper plates and their thermal conductivity and TCR were measured using a custom-built guarded-hot plate apparatus under vacuum conditions. The two-thickness method was used to de-convolute the TCR between the adsorbent layer and the copper plate from the thermal conductivity measurements. The experimental data showed that the thermal conductivity of silica gel-PVP adsorbent was 0.26 W/m/K, i.e., 78.6% higher than that of packed bed of dry silica gel. Also, the results indicated that the $TCR_{ads-metal}$ varied between 1.29–3.80 K/W which is equal to silica gel-PVP adsorbent with 0.2–0.69 mm in thickness. Besides, our measurements showed that the two TCRs between the adsorbent and metallic substrate, $TCR_{ads-metal}$, can be up to 26% of the bulk resistance of the adsorbent-metallic composite.

Acknowledgement

The authors gratefully acknowledge the financial support of the Natural Sciences and Engineering Research Council of Canada (NSERC) through the Automotive Partnership Canada Grant No. APCPJ 401826-10.

References

[1] Motor vehicle fuel consumption and travel in the U.S., 1960–2006, U.S. Dep. Transp., 2006.
[2] T.J. Hendricks, Optimization of vehicle air conditioning systems using transient air conditioning performance analysis, in: SAE Conf. Proc. P, 2001.
[3] R. Farrington, J. Rugh, Impact of vehicle air-conditioning on fuel economy, tailpipe emissions, and electric vehicle range, in: Proceeding Earth Technol. Forum, Washington, D.C., 2000.
[4] L.Z. Zhang, L. Wang, Performance estimation of an adsorption cooling system for automobile waste heat recovery, Appl. Therm. Eng. 17 (1997) 1127–1139.
[5] Y.Z. Lu, R.Z. Wang, S. Jianzhou, M. Zhang, Y. Xu, J. Wu, Performance of a diesel locomotive waste-heat-powered adsorption air conditioning system, Adsorption 10 (2004) 57–68.
[6] M. Verde, L. Cortés, J.M. Corberán, A. Sapienza, S. Vasta, G. Restuccia, Modelling of an adsorption system driven by engine waste heat for truck cabin A/C. Performance estimation for a standard driving cycle, Appl. Therm. Eng. 30 (2010) 1511–1522.
[7] H. Demir, M. Mobedi, S. Ülkü, A review on adsorption heat pump: Problems and solutions, Renew. Sustain. Energy Rev. 12 (2008) 2381–2403.
[8] F. Poyelle, J.J. Guilleminot, F. Meunier, Experimental tests and predictive model of an adsorptive air conditioning unit, Ind. Eng. Chem. Res. 38 (1999) 298–309.
[9] Z. Tamainot-Telto, R.E. Critoph, Monolithic carbon for sorption refrigeration and heat pump applications, Appl. Therm. Eng. 21 (2001) 37–52.
[10] A. Freni, M.M. Tokarev, G. Restuccia, A.G. Okunev, Y.I. Aristov, Thermal conductivity of selective water sorbents under the working conditions of a sorption chiller, Appl. Therm. Eng. 22 (2002) 1631–1642.
[11] A. Sharafian, M. Bahrami, Adsorbate uptake and mass diffusivity of working pairs in adsorption cooling systems, Int. J. Heat Mass Transfer 59 (2013) 262–271.
[12] H. Bjurström, E. Karawacki, B. Carlsson, Thermal conductivity of a microporous particulate medium: moist silica gel, Int. J. Heat Mass Transfer 27 (1984) 2025–2036.
[13] C.L. Mantell, Adsorption, 2nd ed., McGraw-Hill, New York, 1951.
[14] W. Niebergall, Arbeitsstoffpaare für Sorptions-Kältemaschinen, Sorptions-Kältemaschinen. 7 (1959) 119–164.
[15] S.Z. Vasil'ev, V.I. Letichevskii, V.L. Mal'ter, M.Y. Solntsev, G.M. Yusova, O.M. Kostenok, et al., The effective thermal conductivity of zeolite and silica gel layers, Chem. Pet. Eng. 15 (1979) 33–35.
[16] C.S. Sharma, P. Harriott, R. Hughes, Thermal conductivity of catalyst pellets and other porous particles: Part II: Experimental measurements, Chem. Eng. J. 10 (1975) 73–80.
[17] C.S. Sharma, R. Hughes, The thermal conductivity of porous catalyst compacts, Can. J. Chem. Eng. 54 (1976) 358–363.

[18] H. Blasinski, A. Heim, The influence of porosity on the thermal conductivity of granular layers, Zesz. Nauk. Politech. Łódzkiej – Chem. 24 (1973) 91–106.

[19] L.K. Simonova, Determination of thermal constants of samples of activated carbon and silica gels, Zhurnal Prikl. Khimii. 16 (1943) 87–94.

[20] K. Fujioka, K. Hatanaka, Y. Hirata, Composite reactants of calcium chloride combined with functional carbon materials for chemical heat pumps, Appl. Therm. Eng. 28 (2008) 304–310.

[21] S.E. Gustafsson, E. Karawacki, M.N. Khan, Transient hot-strip method for simultaneously measuring thermal conductivity and thermal diffusivity of solids and fluids, J. Phys. D. Appl. Phys. 12 (1979) 1411–1421.

[22] M. Sarwar, P. Majumdar, Thermal conductivity of wet composite porous media, Heat Recover. Syst. CHP. 15 (1995) 369–381.

[23] G. Dul'Nev, Heat transfer through solid disperse systems, J. Eng. Phys. Thermophys. 9 (1965) 399–404.

[24] A.V. Luikov, A.G. Shashkov, L.L. Vasiliev, Y.E. Fraiman, Thermal conductivity of porous systems, Int. J. Heat Mass Transfer 11 (1968) 117–140.

[25] Y.Y. Tanashev, Y.I. Aristov, Thermal conductivity of a silica gel+ calcium chloride system: the effect of adsorbed water, J. Eng. Phys. Thermophys. 73 (2000) 876–883.

[26] Y.Y. Tanashev, A.V. Krainov, Y.I. Aristov, Thermal conductivity of composite sorbents "salt in porous matrix" for heat storage and transformation, Appl. Therm. Eng. 61 (2013) 401–407.

[27] H.T. Chua, K.C. Ng, A. Chakraborty, N.M. Oo, M.A. Othman, Adsorption characteristics of silica gel + water systems, J. Chem. Eng. Data. 47 (2002) 1177–1181.

[28] B.B. Saha, A. Chakraborty, S. Koyama, Y.I. Aristov, A new generation cooling device employing CaCl2-in-silica gel–water system, Int. J. Heat Mass Transfer 52 (2009) 516–524.

[29] R.E. Critoph, Y. Zhong, Review of trends in solid sorption refrigeration and heat pumping technology, Proc. Inst. Mech. Eng. Part E J. Process Mech. Eng. 219 (2005) 285–300.

[30] S. Mauran, P. Prades, F. L'Haridon, Heat and mass transfer in consolidated reacting beds for thermochemical systems, Heat Recover. Syst. CHP. 13 (1993) 315–319.

[31] M. Pons, D. Laurent, F. Meunier, Experimental temperature fronts for adsorptive heat pump applications, Appl. Therm. Eng. 16 (1996).

[32] L. Marletta, G. Maggio, A. Freni, M. Ingrasciotta, G. Restuccia, A non-uniform temperature non-uniform pressure dynamic model of heat and mass transfer in compact adsorbent beds, Int. J. Heat Mass Transfer 45 (2002) 3321–3330.

[33] T. Miltkau, B. Dawoud, Dynamic modeling of the combined heat and mass transfer during the adsorption/desorption of water vapor into/from a zeolite layer of an adsorption heat pump, Int. J. Therm. Sci. 41 (2002) 753–762.

[34] T. Eun, H. Song, J. Hun, K. Lee, J. Kim, Enhancement of heat and mass transfer in silica-expanded graphite composite blocks for adsorption heat pumps: Part I. Characterization of the composite blocks, Int. J. Refrig. 23 (2000) 64–73.

[35] T. Eun, H. Song, J. Hun, K. Lee, J. Kim, Enhancement of heat and mass transfer in silica-expanded graphite composite blocks for adsorption heat pumps. Part II. Cooling system using the composite blocks, Int. J. Refrig. 23 (2000) 74–81.

[36] X. Zheng, L.W. Wang, R.Z. Wang, T.S. Ge, T.F. Ishugah, Thermal conductivity, pore structure and adsorption performance of compact composite silica gel, Int. J. Heat Mass Transfer 68 (2014) 435–443.

[37] L.W. Wang, Z. Tamainot-Telto, S.J. Metcalf, R.E. Critoph, R.Z. Wang, Anisotropic thermal conductivity and permeability of compacted expanded natural graphite, Appl. Therm. Eng. 30 (2010) 1805–1811.

[38] L.W. Wang, Z. Tamainot-Telto, R. Thorpe, R.E. Critoph, S.J. Metcalf, R.Z. Wang, Study of thermal conductivity, permeability, and adsorption performance of consolidated composite activated carbon adsorbent for refrigeration, Renew. Energy 36 (2011) 2062–2066.

[39] ASTM C177-13, Standard Test Method for Steady-State Heat Flux Measurements and Thermal Transmission Properties by Means of the Guarded-Hot-Plate Apparatus, ASTM Int., 2004.

[40] E. Sadeghi, S. Hsieh, M. Bahrami, Thermal conductivity and contact resistance of metal foams, J. Phys. D. Appl. Phys. 44 (2011) 125406.

[41] E. Sadeghi, N. Djilali, M. Bahrami, Effective thermal conductivity and thermal contact resistance of gas diffusion layers in proton exchange membrane fuel cells. Part 1: Effect of compressive load, J. Power Sources 196 (2011) 246–254.

[42] G. Unsworth, N. Zamel, X. Li, Through-plane thermal conductivity of the microporous layer in a polymer electrolyte membrane fuel cell, Int. J. Hydrogen Energy 37 (2012) 5161–5169.